# Multi-target electrochemical malaria aptasensor on flexible multielectrode arrays for detection in malaria parasite blood samples

Gabriela Figueroa-Miranda[a,b], Song Chen[a,b], Marc Neis[a], Lei Zhou[a,b], Yuting Zhang[a], Young Lo[c], Julian Alexander Tanner[c], Andrea Kreidenweiss[d,e], Andreas Offenhäusser[a], Dirk Mayer[a*]

[a]Institute of Biological Information Processing, Bioelectronics (IBI-3), Forschungszentrum Jülich GmbH, Jülich, Germany

[b]RWTH Aachen University, Aachen, Germany

[c]School of Biomedical Sciences, Li Ka Shing Faculty of Medicine, The University of Hong Kong, Pokfulam, Hong Kong Special Administrative Region

[d]Institute of Tropical Medicine, University of Tübingen, Tübingen, Germany

[e]Centre de Recherches Médicales de Lambaréné (CERMEL), Lambaréné, Gabon

*Corresponding author: Dirk Mayer

Address: Institute of Biological Information Processing, Bioelectronics (IBI-3), Forschungszentrum Jülich GmbH, Wilhelm-Johnen-Straße 52428, Jülich, Germany

Email: dirk.mayer@fz-juelich.de

Tel.: +49-2461-61-4023

## Abstract

Despite all efforts, malaria is still highly prevalent in tropical and developing countries. The "test, treat and track" policy of the World Health Organization (WHO) demands the development of affordable and highly sensitive malaria tests that discriminate between the two common malaria parasites, *Plasmodium falciparum* and *Plasmodium vivax*, to guide appropriate treatments. In response, we developed a flexible and disposable multielectrode array utilized as electrochemical malaria aptasensor. This multi-target aptasensor was modified by four different aptamer receptors, discriminating between *P. falciparum* and *P. vivax* infections via *Plasmodium* lactate dehydrogenase, expressed by both species, and histidine-rich protein 2, exclusively expressed by *P. falciparum*. The multi-target aptasensor detection was tested in blood samples spiked with target proteins, whole human blood spiked with *P. falciparum*, and *P. falciparum in vitro* cultures. A rigorous analysis revealed sensitivities of >75.0% for 0.001% parasitemia (50 parasites/µL) and a logic gate-based discrimination of

*Plasmodium* infections, overcoming WHO standards. A cost analysis further substantiated the applicability of this multi-target aptasensor as a disposable point-of-care test for remote areas dealing with prevalent malaria parasite infections.

**Keywords:** Flexible polymer substrate; Multielectrode arrays; Multi-target detection; Malaria detection; Electrochemical aptasensor; Blood samples.

## 1. Introduction

Malaria, a vector-borne disease caused by *Plasmodium* parasites, is one of the oldest infectious diseases and continues to cause hundreds of thousands of deaths annually [1]. Tropical and developing countries are most affected by this parasitic disease due to their poor healthcare infrastructure, leading to difficulties in controlling and preventing malaria. With early treatment, *Plasmodium* infections can be completely cured [2, 3]. Therefore, the World Health Organization (WHO) strongly advocates its policy of "test, treat and track" for improving the quality of care and surveillance of malaria prevalence. Furthermore, WHO recommends that all suspected malaria cases should be confirmed by diagnostic testing before treatment is administered to prevent parasite resistance development [4]. It is, therefore, crucial to confirm and discriminate between the two main malaria parasite species, *Plasmodium falciparum* and *Plasmodium vivax,* for correctly guiding treatment options and the rational use of antimalarial medicines [3, 5]. In Africa, more than 90% of all malaria cases are due to *P. falciparum*, while in South-East Asia and the Americas, both *P. falciparum* and *P. vivax* infections are almost equally prevalent. *P. falciparum* is potentially deadly if not treated promptly and effectively [2, 3], whereas *P. vivax* is less virulent, but can cause relapse by dormant forms residing in the liver that requires specific treatment [1].

Many commercially available rapid diagnostic tests (RDTs) are on the market for the detection of malaria parasites. Their detection is based on monoclonal antibodies serving as receptor molecules specifically binding to a *Plasmodium* antigen. Unfortunately, such commercial RDTs still lack analytical sensitivity, and the majority of WHO recommended RDTs can detect only *P. falciparum*, with a few tests also targeting *P. vivax* [6-10]. Besides, the receptor antibodies have reduced thermostability at higher temperatures, considerable production costs, and have limited potential for chemical modifications to directly adapt towards other diagnostic platform technologies. In this regard, more robust detection molecules like aptamers are promising alternatives to improving malaria diagnosis [11]. An aptamer, a short single-stranded oligonucleotide sequence, binds to a target analyte with high specificity. Compared to antibodies, aptamers are thermostable, small, affordable, easily synthesized, and readily chemically modified. Hence, aptamers can overcome the difficulties associated with antibody-based tests [6]. Several detection technologies applying different transducers, ranging from optical to electrochemical, have been proposed by implementing aptamers as receptor molecules [6, 8, 12-16].

The reported aptamer-based detection systems mainly sense protein biomarkers since they are upregulated for the demanding metabolic rate of the infecting *Plasmodium* parasites. One of the main proteins for malaria diagnosis is the essential energy-converting enzyme *Plasmodium* lactate dehydrogenase (PLDH), expressed by all malaria parasite species [8, 17, 18]. Another commonly used biomarker is *P. falciparum* histidine-rich protein 2 (PfHRP-2 or HRP-2), which is an abundant protein exclusively expressed by *P. falciparum* parasites. It is present in red blood cells, serum, cerebrospinal fluid, and urine of *P. falciparum*-infected patients [7, 17]. Concentration levels of both antigens correlate with parasitemia and can thus reflect parasite levels [8, 17, 18]. A combination of receptors in a diagnostic device simultaneously targeting these two main malaria biomarkers could be of great advantage in discriminating between *P. falciparum* and *P. vivax* parasites.

Among the different implemented detection techniques, electrochemical sensors have demonstrated their strengths regarding high sensitivity, straightforward operation and detection, device miniaturization, integration in microsystems, and thus point-of-care applications [12]. A promising electrochemical sensor platform is multielectrode array (MEA), which combines the advantages of integrating multiple, individually addressable sensor electrodes on a small lateral footprint, with fast electrode kinetics, and low-noise recording capabilities [19]. For some decades, the MEA approach has been mainly used to detect physiological activity in cellular networks [20-24] and nanoparticle impact detection [19, 25]. Recently, MEAs are increasingly used for multi-target electrochemical biosensing [26-31]. The fabrication of a multi-target biosensor has been realized on rigid substrates like quartz or silicon by immobilizing, on the same electrode, two different labeled aptamers with two different redox reporters [27]. Another approach was implementing electrochemical lithography to remove some previously immobilized aptamers and subsequent immobilization of a second receptor [31]. The commonly implemented method for different receptor immobilization is by drop-casting on flexible substrates, which usually requires big fabricated electrodes to avoid cross-contamination of drops [26, 28, 29]. The manufacturing of MEAs on soft polymer substrates promises lower fabrication costs, and flexibility compliant to the mechanical tension of the biological matter [32-34]. It also realizes the ease of a multi-target biosensor by allowing individually addressable set of electrodes to be incubated in different solutions, a characteristic that has not been exploited so far.

Here, we report a flexible multielectrode array (flex-MEA) and multi-target electrochemical malaria aptamer-based biosensor (aptasensor). The polymer-based flex-MEA facilitates the

immobilization of different aptamers by multiple, individually addressable electrodes, providing the possibility to discriminate between the *P. falciparum* and *P. vivax* infection. Here, *Plasmodium* detection is achieved by immobilizing four distinct and specific aptamers on separate electrodes on the same sensor chip: i) the 2008s aptamer, previously electrochemically characterized for its binding to *P. falciparum* lactate dehydrogenase (PfLDH) [15, 16, 35]; ii) the pL1 aptamer, which binds to both PfLDH and *P. vivax* LDH (PvLDH) [36]; iii) the LDHp11 aptamer, highly and exclusively selective for PfLDH [37]; and iv) the 2106s aptamer, which selectively detects HRP-2 protein [38, 39]. The combination of different output signals from the different receptors immobilized on separate electrodes can be operated as logic gates for specific parasite detection. This flex-MEA multi-target aptasensor was first characterized using blood samples spiked with recombinant *Plasmodia* proteins. Then, it was challenged with *P. falciparum* parasitized blood, where the flex-MEA multi-target aptasensor also confirmed its highly sensitive, specific, and selective performance.

## 2. Experimental section

### *2.1. Materials and reagents*

All *Plasmodia* antigen-binding single-stranded DNA (ssDNA) aptamer sequences and control random ssDNA sequences were synthesized by Friz Biochem GmbH (Neuried, Germany), which are shown in Table S4. The recombinant *Plasmodium falciparum* lactate dehydrogenase (PfLDH), *Plasmodium vivax* lactate dehydrogenase (PvLDH), *Plasmodium falciparum* histidine-rich protein 2 (HRP-2), and human lactate dehydrogenase (hLDH) were obtained from bacterial expression [11]. Monofunctional methoxy- polyethylene glycol thiol (PEG, 2kDa) was purchased from Creative PEGWorks (New York, USA). 25 mM Tris-HCl buffer (NaCl 0.1 M, Tris 25 mM, HCl 25 mM, pH 7.5), lysis buffer (25 mM Tris-HCl buffer with 0.5% Triton X-100), high salt concentration phosphate-buffered saline (PBS, 10 mM sodium phosphate with 1 M NaCl and 1 mM $Mg^{2+}$, pH 7.5), 0.1 M NaOH solution, and 0.05 M $H_2SO_4$ solution were prepared. All aqueous solutions were prepared using ultra-pure deionized water (18.2 MΩ cm, Milli-Q, Millipore, Merck, Darmstadt, Germany). Tris (2-carboxyethyl) phosphine hydrochloride (TCEP), potassium ferricyanide ($K_3[Fe(CN)_6]$), potassium ferrocyanide ($K_4[Fe(CN)_6]$) trihydrate were purchased from Sigma-Aldrich Chemie GmbH (Germany). Ethanol and isopropanol were purchased from Merck (Darmstadt, Germany).

*2.2. Flexible multielectrode array fabrication and cleaning*

Flexible multielectrode arrays (flex-MEAs) were produced in an ISO 1-3 cleanroom on a polyethylene terephthalate (PET, DuPont Teijin Films Ltd) foil with a thickness of 100 µm and a diameter of 100 mm used as flexible substrate. Before the deposition of the metals, a rigorous substrate cleaning utilizing acetone and isopropanol was performed for the removal of dust particles (Fig. S1a and b). A physical vapor deposition (PVD) process was performed to obtain a 5 nm titanium (Ti) adhesion layer and the 50 nm gold for the electrode's fabrication (Pfeiffer PLS 570, Pfeiffer Vacuum, Asslar, Germany). The feedlines and the 20 patterned electrodes were defined firstly via standard photolithography using the Mask aligner (MA4, Süss MicroTec). Afterwards, a wet chemical etching procedure was performed to remove the excess of gold using gold etchant (TechniEtch ACl2, Microchemicals, Ulm, Germany), followed by an additional wet chemical etching step to remove also the Ti by means of a titanium etchant (TechniEtch TC, Ulm, Germany). The photoresist layer was stripped by immersing the PET substrate with the patterned electrodes in acetone for 10 min, followed by isopropanol and DI-water rinsing.

For the deposition of a Parylene-C passivation layer, the polymer tape ELEP HOLDER BT-150E (Nitto, Japan) was used to fabricate a stencil utilizing a laser cutting machine (Glowforge basic, Seattle, USA). Then the stencil was adhered to the PET substrate with the patterned electrodes. Afterwards, the deposition of Parylene-C was performed by low-pressure chemical vapor deposition (LPCVD) with the following parameters: Vacuum PLA1 20, SP 25, and Vaporizor PhA1 160 (SCS Labcoater (PDS 2010), KISCO, Indianapolis, USA). Finally, the stencil was peeled off carefully from the PET substrate (See Fig. S1c). The obtained flexible polymer chips had a size of 10.5 mm × 21.5 mm, with 20 individually addressable electrodes (Fig. S1d).

For final cleaning before usage, the new flex-MEA chips were immersed in acetone, and isopropanol for 5 minutes each, followed by Milli-Q water rinsing and drying in a nitrogen flow. The chemically cleaned electrodes were connected to a printed circuit board (PCB, Würth Electronic GmbH & Co. KG) with a zero insertion force (ZIF) connector that allowed the enlace to the potentiostat (Fig. S1d). The electrochemical cleaning of the flex-MEA chip was performed by cyclic voltammetry (CV) first in 0.1 M NaOH with a potential range from −1.35 V to −0.35 V during 10 scans at 2 V $s^{-1}$, and subsequently scanning in 0.05 M $H_2SO_4$ with a

potential range from 0 V to 1.5 V during 20 scans at 1 V $s^{-1}$ (Zhang *et al*. 2020). The electrochemical surface area (ESA) was determined by CV in 0.05 M $H_2SO_4$ in a potential range from 0 V to 1.5 V at 0.1 V $s^{-1}$ [40].

### *2.3. flex-MEA multi-target aptasensor biofunctionalization*

The optimized concentrations of the ssDNA aptamers were 0.5 µM for 2008s, pL1, and 2106s, and 0.03 µM for LDHp11 (Fig. S3). All aptamers were incubated separately with 10 mM TCEP solution for 1 h at room temperature to break the disulfide-protecting bond and permit the immobilization of the aptamer-thiol /gold self-assembled monolayer. After the specified time, the solutions were resuspended in 10 mM high salt concentration PBS buffer to a final volume of 1 mL. The flex-MEA was partially cut in four parallel stripe-like sections by scissors before the incubation with the aptamer solutions (Fig. 1a), maintaining the electrodes and feedlines unaffected as corroborated by their calculated electroactive surface area (ESA, Fig. S2 and Table S1). This partially cut flex-MEA facilitated the incubation of separate sets of electrodes individually with the four different aptamer solutions stored in separate vials for the final generation of the multi-target aptasensor. The individual immobilization approach ensured that every type of aptamer was tethered to a separate set of electrodes and that every electrode is functionalized only with on kind of receptor. The electrodes were incubated overnight in the dark with the respective aptamer solution. The aptamer-modified flex-MEAs were then rinsed with Tris buffer and consecutively with Milli-Q water to remove unspecific adsorbed molecules. Subsequently, the flex-MEAs were immersed in a 5 mg/mL PEG solution for 7 h. The PEG was used as a blocking molecule to avoid biofouling from other molecules present in the blood samples [15]. Finally, the flex-MEA aptasensor was rinsed with Tris buffer to remove excess unspecific adsorbed PEG molecules.

### *2.4. flex-MEA electrochemical multi-target aptasensor detection in blood samples*

The functionality of the flex-MEA aptasensor was tested using positive control samples, which were blood spiked with the respective recombinant target proteins, either PfLDH, PvLDH, or HRP-2. Therefore, the aptasensor was immersed in 2 mL blood samples diluted 1:100 in 25 mM Tris buffer containing the respective spike protein at concentrations between 100 fM to 100 nM for 45 min. After rinsing, the aptasensor was subsequently immersed in 5 mM $[Fe(CN)_6]^{3-/4-}$ in

Tris buffer solution to record differential pulse voltammetry (DPV) curves. In the same way, the control test with hLDH was performed.

*P. falciparum* strain 3D7 cultures (BEI Resources) were propagated *in vitro* in O+ erythrocytes at haematocrit of 2.5% (Tübingen University Hospital´s blood bank) and medium as described earlier [41]. *In vitro* cultures containing mixed parasite life cycle stages were used for the assays. For pure *P. falciparum* parasite *in vitro* cultures, the parasitemia was adjusted accordingly with infected red blood cells. For samples mimicking a malaria patient, human whole blood samples were spiked with *P. falciparum* cultures to achieve also the required parasitemia with infected red blood cells. Uninfected red blood cells in medium and in whole blood samples were used as respective negative controls. On the day of the assay performance, samples were thawed at room temperature and mixed 1:1 with lysis buffer. After 15 min incubation with the buffer, the resulting lysed parasitized blood was diluted 1:100 in Tris buffer. The multi-target aptasensor detection was performed in the same way as previously described by DPV measurements of spiked blood.

The DPV measurements were carried out with a multichannel CHI1030B potentiostat (Austin, USA) with a three-electrode system. Thus, a platinum wire was utilized as the counter electrode (CE), an Ag/AgCl electrode (DriRef2, WPI, Germany) as the reference electrode (RE), and the flex-MEA multi-target aptasensor was operated as the working electrode (WE). DPV measurements were carried out at a potential range lasting from 0 to 0.7 V with a step potential of 0.005 V, modulation amplitude of 0.025 V, an equilibration time of 2 s, a pulse width of 0.05 s, and a sampling width of 0.025 s.

## 3. Results and Discussion

### *3.1. flex-MEA mechanical characterization showed its robustness*

Gold multielectrode array chips, which possess 20 individually addressable gold electrodes (550 µm x 550 µm), were fabricated on a flexible polyethylene terephthalate (PET) substrate with a calculated surface roughness of 1.41±0.27 nm (Fig. S1b). The implemented flexible PET polymer substrate allowed to partially divide the flex-MEA chip into four sets of electrodes (Fig. 1a). The flex-MEA robustness was evaluated by a mechanical bending test, demonstrating that they withstand multiple bending cycles without apparent electrochemical performance changes. To perform the mechanical bending, the flex-MEA was fixed to the top and bottom

clamps of a tailor-made linear translation stage (Fig. 1b). Only the upper clamp was moved downwards with a speed of 150 mm/min and retracted back to its original position, counting this movement as a full bending cycle. After finalizing a set of specified bending cycles (5, 25, 75, 175, 425, 925, and 1925), the electrochemical performance of the electrodes was evaluated. As shown in Fig. 1c, the cyclic voltammogram recorded in 5 mM $[Fe(CN_6)]^{3-/4-}$ solution remained almost unaltered with less than 5 % peak current deviation. The calculated electroactive surface area (ESA, Fig. S2 and Table S1) confirmed the sensor stability with a calculated value quite close to its original 100 % even after 925 bending repetitions (Fig. 1d). After 1925 bending cycles, a slight increment of the area was observed (106.3 ± 1.8 %), which might be associated to the formation of minor cracks or a slight delamination of the dielectric cover exposing additional parts of the electrode leads to the electrolyte. However, with this high number of withstood bending cycles, the flex-MEA electrodes proved to be very resistant to harsh continuous mechanical distortions.

The implemented simple stencil passivation with Parylene-C polymer (Fig. S1c) gives an extra advantage in the production cost over the commonly used cleanroom-based lithographic passivation, which required the utilization of several additional processing steps and reagents (Table S2). The cost of the stencil passivation process was 58 % lower in comparison to the lithographic passivation, in addition to the lower price of the flexible PET substrate over silicon or quartz (Table S3).

<Fig. 1 here>

*3.2. Performance in blood with spiked target proteins*

The partially divided four sets of electrodes of the flex-MEA chip allows incubating individual sets of electrodes with different aptamer solutions to realize a label-free, multi-target analyte detection of PfLDH and HRP-2 malaria biomarkers (Fig. 2). The sequences of the used aptamers are shown in Table S4.

<Fig. 2 here>

Calibration curves were recorded for all 4 aptamer receptors to quantify the detection capability of each aptasensor from multiple electrodes located on several flex-MEA chips. Therefore, the chips were incubated for 45 min in the analyte solution containing the biomarker at a given concentration. This incubation time was chosen since the signal reached a stable plateau after this time (Fig. S4) facilitating a stable quantitative detection. A qualitative detection would be

possible by our multi-target aptasensor already after 10 to 15 min similar to other reported qualitative detection methods (see Table S5). Compared to other quantitative assays such as ELISA or ELONA, our biosensor showed a faster detection performance.

The current change ($\Delta I$) induced by the aptamer-protein binding was determined in the redox probe solution by means of DPV measurements (Fig. 2). The obtained calibration curves were fitted by a Langmuir-Freundlich adsorption isotherm formula (equation 1) [42] to quantitatively characterize the analyte binding of the different aptamers (Fig. 3),

$$\frac{\Delta I}{I_0} = \frac{\left(\frac{\Delta I}{I_0}\right)_{max} \cdot k_{eq} \cdot c^n}{1 + k_{eq} \cdot c^n} \quad (1)$$

where $I_0$ stands for the peak current measured before protein administration and $\Delta I$ the change of peak current after the addition of protein (Fig. 2). $(\Delta I / I_0)_{max}$ is the maximum possible signal obtained, $k_{eq}$ the equilibrium constant, $c$ the protein concentration, and $n$ the homogeneity coefficient with a value between 0 and 1. The calculated limit of detection (LOD), obtained as three times the standard deviation of the normalized electrochemical signal from the blank, and other obtained performance factors are summarized in Table 1 for each aptamer. The aptamer surface densities were optimized in advance to get higher signals for detection of the respective analytes (Fig. S3).

The 2008s aptamer (Fig. 3a, Table 1), which targets PfLDH, had a calculated LOD value of 7.25 fM. The maximum signal obtained $(\Delta I / I_0)_{max}$ from the fitting to the experimental data was 12.1, correlating with the observed saturation reached at 100 nM PfLDH. Thus, the aptasensor showed a semi-logarithmic dynamic detection range lasting from 7.25 fM to 10 nM. This flex-MEA aptasensor demonstrated an improved LOD of two orders of magnitude compared with a previously reported impedimetric system utilizing 2008s aptamers on a single gold rod electrode tested in human serum samples [15]. Interestingly, a cross-selectivity of 2008s aptamer towards PvLDH and HRP-2 was observed (Fig. 4a), likely due to sequence similarity with PfLDH and reported binding to the histidine tag [11], respectively. Another employed aptamer was pL1 (Fig. 3b), which targets PfLDH and PvLDH [36]. The corresponding aptasensor possessed a LOD of 22.3 fM and a similar sensitivity as the 2008s aptamer (2.1 ± 0.2 /decade) (Table 1). The $(\Delta I / I_0)_{max}$ was 15.0, which was close to the highest (100 nM) PfLDH concentration tested. The semi-logarithmic dynamic detection range for this aptasensor lasted from 22.3 fM to 100 nM. Although this aptamer is reported to target also PvLDH, in the cross-selectivity results, there was a smaller signal response for this protein

(LOD = 138 pM) (Fig. 4b). This might be due to the different pH conditions (8.0) used in the previously published assay. It is well established that differences in experimental conditions such as pH can influence the kinetics of aptamer-target binding [36, 37]. In this work, physiological pH conditions (7.5) were chosen to be compatible with real blood samples. Furthermore, we reported recently that the backfill molecule can affect the detection limit and the dynamic detection range [15]. Although different backfill molecules where used here (PEG) in comparison with previous studies (mainly mercapto hexanol), it remains generally unknown how the backfill influences the cross-selectivity of electrochemical aptamer sensors. Interestingly, a cross-selectivity for HRP-2 was also observed (Fig. 4b). Also here, the high density of histidines in the protein sequence and the affinity tag of these biomarkers (PfLDH, PvLDH and HRP-2) may cause this cross-selectivity.

<Fig. 3 here>

The third characterized receptor was the LDHp11 aptamer (Fig. 3c), which was reported to target exclusively PfLDH [37]. Our study corroborated such specific detection for PfLDH over PvLDH and HRP-2 proteins (Fig. 4c). The calculated LOD = 1.80 fM was higher compared with the previous aptasensors, but with similar sensitivity S = 2.5 ± 0.1 / decade and with a $(\Delta I/I_0)_{max}$= 17.2, close to the highest (100 nM) PfLDH concentration tested. For this aptasensor, the semi-logarithmic concentration-range lasted from 1.80 fM to 100 nM.

In general, the LODs and dynamic detection ranges of the three aptamers targeting PfLDH (2008s, pL1, and LDHp11) complemented each other and possessed excellent sensitivity similar to other reported state-of-the-art sensors [6, 12]. Noteworthy, the utilization of several aptamers with different binding affinities (Table S6) that target different epitopes of the same LDH protein forming different secondary structures [11, 36, 37] contributes to higher reliability of the analysis of patient samples. Furthermore, the different PfLDH receptors possessed different selectivity for PvLDH. The latter two aspects can be utilized to logic gate operations to better evaluate the sample composition, as explain below.

<Table 1 here>

The fourth characterized receptor was the 2106s aptamer (Fig. 3d), which forms a stem-loop secondary structure (Fig. S5) binding to HRP-2 protein, exclusively expressed by *P. falciparum* parasites [38]. HRP-2 was detected at a low LOD of 0.15 pM, and with a high sensitivity (see Table 1). The maximum calculated signal $(\Delta I/I_0)_{max}$ was 21.9, which was even beyond the

here tested concentration range (100 nM). This aptasensor demonstrated excellent detection performance similar to previously reported electrochemical aptasensors targeting HRP-2 [6, 8, 12, 39]. The cross-selectivity to PfLDH and PvLDH was lower as compared with its target (Fig. 4d). All aptamers were checked for their binding capability towards the human lactate dehydrogenase (hLDH), which is intrinsically present in human blood samples (Fig. 4). The flex-MEA multi-target aptasensor showed a smaller unspecific signal for hLDH than its specific targets for all receptor aptamers. In order to take advantage of the different specific (single target detection) and selective (several targets) signal outputs from different receptors [43], the combination of the different outputs can be processed as logic gates [44, 45]. As shown in Table S7, a detection via a single aptasensor could lead to unclear sensor outputs due to the cross-selectivity for certain sample compositions containing several target biomarkers. Despite of the observed cross-selectivity, the detection of specific parasitemia infections can be achieved by combining the signal outputs from different aptamers operated as logic gates. These logic gates facilitates an unambiguous detection of malaria infections, discriminating between these two main malaria parasites, confirming the result by averaging over several redundant sensor signals and discarding the possibility of a false-positive result. An example of such logic gate operation for the specific confirmation of *Plasmodium falciparum* infection is shown in Table 2 and 3.

<Table 2 here>

<Table 3 here>

As shown in the example of Table 2, the sensor signal from LDHp11 and 2106s aptasensors are used as inputs of an AND gate, which computes a positive (1) signal output (indicating a *P. falciparum* infection) only in the presence of both specific biomarkers (PfLDH and HRP-2), (Table 3). The gate input (sensor signal) is considered as being 0 or 1 if the measured current is below or above the LOD threshold, respectively (Fig. 3). Therefore, in this specific case the combination of LDHp11 and 2106s aptasensors detect and confirm *P. falciparum* infections via redundant PfLDH and HRP-2 biomarker signals. Two additional examples of logic gates are provided in the SI, one in Table S9 for the specific detection of *Plasmodium vivax* by a combination of output signals from 2008s, LDHp11 and 2106s aptamers (Table S8), and the second in Table S11 for redundant signal detection by a combination of output signals from 2008s and pL1 aptamers (Table S10), discarding with this last example the possibility of a false-positive result. Noteworthy, this is just a small selection among all possible and potentially useful logic gates that could be realized out of the four aptasensors integrated on the flex-MEA chip.

A recent study reported by Jimenez *et al.* calculated the analytical sensitivity of the classified best-in-class malaria RDTs according to WHO by a comparison of quantitative ELISA tests [9]. In that work, the reported detection limits were 25 ng/mL (178 pM) and 0.8 ng/mL (26 pM) for pLDH and HRP-2, respectively. Those values are five and two orders of magnitude higher than the detection limits reported here for this flex-MEA multi-target aptasensor for PfLDH and HRP-2, respectively. The short-term stability of the multi-target aptasensor was tested and demonstrated over a monitored time from 45 min to 7.5 h (Fig. S6a). Only small non-systematic signal alterations (< 10.0 %) were registered for all tested aptamer receptors during this period. However, for a long-term storage (> 1 day) in Tris buffer at 4 °C, a considerable degradation of the signal was observed (Fig. S6b), similar as previously reported for the 2008s aptamer [15]. However, this can be overcome by implementing aptamers with multiple anchoring thiol groups, which can help to reduce the surface diffusion of adsorbed molecules and thus enhance the long-term stability of this multi-target aptasensor [46].

<Fig. 4 here>

*3.3. Performance in P. falciparum blood samples*

The flex-MEA multi-target aptasensor was tested with two types of parasite samples: *P. falciparum in vitro* cultures maintained in concentrated erythrocytes and medium (Fig. 5), and human whole blood samples spiked with *P. falciparum in vitro* cultures to mimic a malaria patient sample (Fig. S7). Both samples were tested at varying parasite densities at levels found in infected individuals. In contrast to *in vitro P. falciparum* cultures kept in erythrocytes, spiked whole blood samples also have leucocytes, platelets, and plasma, potentially interfering with aptamer binding. In both cases, flex-MEA arrays were incubated in lysed *P. falciparum* parasites of all life cycle stages at parasitemia of 0.0001 %, 0.001 %, 0.01 %, 0.1 %, 1 %, and 5 % (<50 – 270000 parasites/µL) [47]. Uninfected erythrocytes (uRBC) were used as the negative control.

The signal response for every single aptasensor (spheres with the same color) of the flex-MEA was considered positive (threshold value), when it was higher than the mean value of the control response + 3σ (Fig. 5). The sensitivity of parasitemia detection for each aptasensor was calculated as the number of positive signal responses among the total number of positive samples. The specificity was determined as the number of negative signals among the total number of negative control samples. For the *P. falciparum* parasite cultures, the 2008s aptamer (threshold value of $(\Delta I/I_0) = 60.0$) had a sensitivity of 83.3 % for a parasitemia of 0.001 % (Fig.

5a and Table S13). For the pL1 aptamer (threshold value of ($\Delta I/I_0$) = 56.6), the sensitivity was 80.0 % for 0.001 % parasitemia (Fig. 5b). The LDHp11 (threshold value of ($\Delta I/I_0$) = 139.3) showed a sensitivity of 80.0 % for 0.0001% parasitemia (Fig. 5c). The 2106s aptamer (threshold value of ($\Delta I/I_0$) = 66.0) demonstrated 83.3 % sensitivity also for 0.001 % parasitemia (Fig. 5d). We determined a limit of detection of 0.001 % parasitemia (50 parasites/µL) for 2008s, pL1, and 2106s, while it was 0.0001 % parasitemia (<50 parasites/µL) for LDHp11. For parasite-infected whole blood samples, the detection limit (>75.0 %) was estimated to 0.01 % parasitemia (500 parasites/µL) with 93.3 %, 100 %, and 100 % of sensitivities, respectively for the 2008s, pL1 and 2106s aptamers (Fig. S7a, c, d and Table S12). For the LDHp11 aptamer, a higher detection limit of 0.1 % parasitemia (5000 parasites/µL) was obtained with 100 % sensitivity (Fig. S7b and Table S12). Thus, this developed flex-MEA multi-target aptasensor fulfills and even overcomes the WHO required detection limit of RDTs of minimum detection of 75.0 % at 200 parasites/µL [10], for simultaneous detection of the biomarker via different aptamers detecting varying epitopes of this target protein. The flex-MEA aptasensor is potentially more sensitive than current RDTs whoever, this needs to be proofed by patient samples in the future [47, 48]. The sensitivities here found with both kinds of samples (>90.0 % for 0.01% parasitemia) were even higher than sensitivities reported for commercial RDTs (<90.0 %) with the same percentage of parasitemia for PfLDH detection [47, 48]. In the case of HRP-2 detection with commercial RDTs, high sensitivities (≈98.0 %) are reported for the same percentage of parasitemia, similar to our detections with 100 % sensitivity [7, 48]. The higher reported half-life stability of HRP-2 compared to PLDH is an important contributor [7]. Since both biomarkers are detected simultaneously, the higher sensitivity for HRP-2 improves the overall clinical assessment of the malaria parasite infection by this test.

<Fig. 5 here>

In the strict sense, the specificities obtained for *P. falciparum* parasite cultures of 83.3 % (2008s), 70.0 % (pL1), 100 % (LDHp11), and 83.3 % (2106s) were higher than those of spiked parasite whole blood samples (≈75.0 % for pL1 and LDHp11, 80.0 % and 85.7 % for 2008 and 2106s) (Table S12 and Table S13). Overall, the specificities of our aptasensors were similar to those of ELISA tests (88.0 %) [2]. Additionally, control experiments demonstrated that specific aptamer sequences obtained higher signals than random ssDNA sequences in both parasitized whole blood and cultured *P. falciparum* samples (Fig. S7 and S8). Even an extra control with receptor-free electrode surfaces blocked only with PEG-molecules was performed, with only minor fouling effects (<20.0 % current change) in blood samples (Fig. S9). A thermal treatment

revealed a high stability of the sensor for temperatures as higher as 45 °C with less than 20 % signal loss for all the different aptamers (Fig. S10). Only for treatments with a temperature of 60 °C, a notorious signal degradation was observed. However, temperatures in the tropical countries hardly exceed 50 °C, therefore the conservation of the sensor performance at 45 °C demonstrated the robustness of this multi-target aptasensor withstanding expected environmental high-temperature conditions.

A cost analysis of the flex-MEA multi-target aptasensor used for a point-of-care detection was estimated and compared with reported prices for commercial RDTs, and other reported developed technologies. As shown in Table S14, the price per test of this fabricated flex-MEA multi-target aptasensor is around the price for the commercial qualitative RDTs and cheaper for some of the other proposed technologies. The electronic module, which is the costly part of this sensor, needs to be purchased one time, and it can be used subsequently for a large number of tests. Thus, the investment of 25 USD can be shared among all those tests making them more affordable.

## 4. Conclusions

A gold multielectrode array chip was fabricated on a flexible PET substrate (flex-MEA) capable of enduring more than 1000 bending cycles without changing its electrochemical performance. The flexible PET substrate allowed to partially separate the MEA chip into four sets of electrodes to facilitate the immobilization of four different aptamer receptors: 2008s, pL1, LDHp11, and 2106s for simultaneous multi-target detection. The first three aptamers target PfLDH and the last one HRP-2, both main malaria biomarkers. The excellent detection performance of this multi-target aptasensor was demonstrated by spiking the protein analytes PfLDH and HRP-2 in blood samples. For both, the obtained detection was highly sensitive in a broad range lasting from 1.80 fM to 100 nM and 0.15 pM to 100 nM, respectively. These detection limits were five and two orders of magnitude smaller for pLDH and HRP-2 detection, respectively, than for the reported commercial best-in-class malaria RDTs. In addition, we observed a noticeable cross-selectivity of the 2008s aptamer for PfLDH, PvLDH, and HRP-2, which has not been reported previously for electrochemical aptasensors. The signal from different electrodes with varying aptamer receptors can be used to perform logic gate operations which help to discriminate between specific parasite infections. The flex-MEA multi-target aptasensors were finally challenged by blood samples with spiked *P. falciparum* parasites in

whole blood and *P. falciparum* parasite *in vitro* cultures with different percentages of parasitemia. The sensitivities obtained for different aptamers outperformed the World Health Organization requirements with values higher than >75.0 % for as low as 50 parasites/µL (0.001 % parasitemia). The specificities obtained were in a similar range as quantitative ELISA tests but with a faster detection time.

To our knowledge, this flex-MEA multi-target aptasensor is the first RDT combining the signal from four different aptamer receptors for malaria parasite detection to provide quantitative signals, high signal redundancy and test reliability together with excellent detection performance in *P. falciparum* samples at low parasite densities. Due to its low fabrication cost and high reliability, we anticipate that our RDT will be a useful diagnostic tool that could improve the diagnosis, disease management, surveillance, and treatment of malaria, particularly in remote and developing areas of the world. Furthermore, it could be expected that the concept of simultaneous detection of multiple biomarkers of the same disease can be easily extended to other illnesses. The partial separation of the polymer-based chip facilitates the convenient immobilization of multiple receptors (not restricted to aptamers) on different (sets of) electrodes of the array without mixing of the receptors, avoiding interfering signals. The low production costs keep the quantitative, multi-receptor approach affordable. The utilization of several receptors that target different epitopes of the same biomarker or the detection of different biomarkers of the same disease contributes to the enhanced reliability of the analysis. Furthermore, the capability to detect several biomarkers permits to distinguish different related pathogens with similar symptoms.

**Acknowledgments**

This research work was supported by the Mexican National Council for Science and Technology and the German Academic Exchange Service (No. 448904). We thank Michael Prömpers for his collaboration in the cost analysis of the flex-MEA fabrication.

**Author contributions**

G. F.-M. designed and conducted experiments, data analysis, writing original draft, and editing. S. C. contributed with the fabrication of the flex-MEA chips, conducted experiments, data analysis, and review the manuscript. M. N. participated in the data analysis, figure design, and review the manuscript. L. Z. contributed with designed of experiments, data analysis, and review and editing of the manuscript. Y. Z. contributed with data analysis, discussion, and

reviewing the manuscript. Y. L. participated with reagents/materials tools and review the manuscript. J. A. T. participated with reagents/materials tools and review the manuscript. A. K. contributed reagents/materials tools, writing original draft, and editing. A. O. contributed to data discussion, review, and editing the manuscript. D. M. participated in design of experiments, data analysis and discussion, and writing original draft and editing.

## References


[1] WHO, World malaria report 2020, World Health Organization: Geneva, Switzerland, (2020).

[2] L.L. Fox, T.E. Taylor, P. Pensulo, A. Liomba, A. Mpakiza, A. Varela, et al., Histidine-Rich Protein 2 Plasma Levels Predict Progression to Cerebral Malaria in Malawian Children With Plasmodium falciparum Infection, The Journal of Infectious Diseases, 208(2013) 500-3.

[3] N.J. White, S. Pukrittayakamee, T.T. Hien, M.A. Faiz, O.A. Mokuolu, A.M. Dondorp, Malaria, The Lancet, 383(2014) 723-35.

[4] WHO, Guidelines for the treatment of malaria. , World Health Organization: Geneva, Switzerland, (2015).

[5] K.R. Tan, P.M. Arguin, Chapter 21 - Malaria Diagnosis and Treatment, in: C.A. Sanford, P.S. Pottinger, E.C. Jong (Eds.), The Travel and Tropical Medicine Manual (Fifth Edition), Elsevier2017, pp. 300-14.

[6] F.D. Krampa, Y. Aniweh, P. Kanyong, G.A. Awandare, Recent Advances in the Development of Biosensors for Malaria Diagnosis, Sensors, 20(2020).

[7] J.C. Mouatcho, J.P.D. Goldring, Malaria rapid diagnostic tests: challenges and prospects, Journal of Medical Microbiology, 62(2013) 1491-505.

[8] K.V. Ragavan, S. Kumar, S. Swaraj, S. Neethirajan, Advances in biosensors and optical assays for diagnosis and detection of malaria, Biosensors and Bioelectronics, 105(2018) 188-210.

[9] A. Jimenez, R.R. Rees-Channer, R. Perera, D. Gamboa, P.L. Chiodini, I.J. González, et al., Analytical sensitivity of current best-in-class malaria rapid diagnostic tests, Malaria Journal, 16(2017) 128.

[10] WHO, Malaria rapid diagnostic test performance: summary results of WHO product testing of malaria RDTs: round 1-8 (2008–2018). World Health Organization: Geneva, Switzerland, (2018).

[11] Y.-W. Cheung, J. Kwok, A.W.L. Law, R.M. Watt, M. Kotaka, J.A. Tanner, Structural basis for discriminatory recognition of Plasmodium lactate dehydrogenase by a DNA aptamer, Proceedings of the National Academy of Sciences, 110(2013) 15967-72.

[12] G. Dutta, Electrochemical biosensors for rapid detection of malaria, Materials Science for Energy Technologies, 3(2020) 150-8.

[13] S. Banerjee, M. Nilsen-Hamilton, Aptamers for Infectious Disease Diagnosis IntechOpen, (2019).

[14] J.D. Ospina-Villa, C. López-Camarillo, C.A. Castañón-Sánchez, J. Soto-Sánchez, E. Ramírez-Moreno, L.A. Marchat, Advances on Aptamers against Protozoan Parasites, Genes, 9(2018) 584.

[15] G. Figueroa-Miranda, C. Wu, Y. Zhang, L. Nörbel, Y. Lo, J. Alexander Tanner, et al., Polyethylene glycol-mediated blocking and monolayer morphology of an electrochemical aptasensor for malaria biomarker detection in human serum, Bioelectrochemistry, (2020) 107589.

[16] B. Lenyk, G. Figueroa-Miranda, I. Pavlushko, Y. Lo, J.A. Tanner, A. Offenhäusser, et al., Dual-Transducer Malaria Aptasensor Combining Electrochemical Impedance and Surface Plasmon Polariton Detection on Gold Nanohole Arrays, ChemElectroChem, 7(2020) 4594-600.

[17] P. Jain, B. Chakma, S. Patra, P. Goswami, Potential Biomarkers and Their Applications for Rapid and Reliable Detection of Malaria, BioMed Research International, 2014(2014) 852645.

[18] L. Vivas, A. Easton, H. Kendrick, A. Cameron, J.-L. Lavandera, D. Barros, et al., Plasmodium falciparum: Stage specific effects of a selective inhibitor of lactate dehydrogenase, Experimental Parasitology, 111(2005) 105-14.

[19] K.J. Krause, A. Yakushenko, B. Wolfrum, Stochastic On-Chip Detection of Subpicomolar Concentrations of Silver Nanoparticles, Analytical Chemistry, 87(2015) 7321-5.

[20] B. Bachmann, N.Y. Adly, J. Schnitker, A. Yakushenko, P. Rinklin, A. Offenhäusser, et al., All-inkjet-printed gold microelectrode arrays for extracellular recording of action potentials, Flexible and Printed Electronics, 2(2017) 035003.

[21] A. Blau, Cell adhesion promotion strategies for signal transduction enhancement in microelectrode array in vitro electrophysiology: An introductory overview and critical discussion, Current Opinion in Colloid & Interface Science, 18(2013) 481-92.

[22] A. Czeschik, A. Offenhäusser, B. Wolfrum, Fabrication of MEA-based nanocavity sensor arrays for extracellular recording of action potentials, physica status solidi (a), 211(2014) 1462-6.

[23] J.K.Y. Law, C.K. Yeung, B. Hofmann, S. Ingebrandt, J.A. Rudd, A. Offenhäusser, et al., The use of microelectrode array (MEA) to study the protective effects of potassium channel openers on metabolically compromised HL-1 cardiomyocytes, Physiological Measurement, 30(2009) 155-67.

[24] C.A. Thomas, P.A. Springer, G.E. Loeb, Y. Berwald-Netter, L.M. Okun, A miniature microelectrode array to monitor the bioelectric activity of cultured cells, Experimental Cell Research, 74(1972) 61-6.

[25] K.J. Krause, N. Adly, A. Yakushenko, J. Schnitker, D. Mayer, A. Offenhäusser, et al., Influence of Self-Assembled Alkanethiol Monolayers on Stochastic Amperometric On-Chip Detection of Silver Nanoparticles, Analytical Chemistry, 88(2016) 3632-7.

[26] W. Gao, S. Emaminejad, H.Y.Y. Nyein, S. Challa, K. Chen, A. Peck, et al., Fully integrated wearable sensor arrays for multiplexed in situ perspiration analysis, Nature, 529(2016) 509-14.

[27] Y. Liu, Y. Liu, Z. Matharu, A. Rahimian, A. Revzin, Detecting multiple cell-secreted cytokines from the same aptamer-functionalized electrode, Biosensors and Bioelectronics, 64(2015) 43-50.

[28] W. Song, H. Li, H. Liang, W. Qiang, D. Xu, Disposable Electrochemical Aptasensor Array by Using in Situ DNA Hybridization Inducing Silver Nanoparticles Aggregate for Signal Amplification, Analytical Chemistry, 86(2014) 2775-83.

[29] R.M. Torrente-Rodríguez, H. Lukas, J. Tu, J. Min, Y. Yang, C. Xu, et al., SARS-CoV-2 RapidPlex: A Graphene-Based Multiplexed Telemedicine Platform for Rapid and Low-Cost COVID-19 Diagnosis and Monitoring, Matter, 3(2020) 1981-98.

[30] C. Wu, A. Offenhäusser, D. Mayer, A Highly Sensitive Amperometric Aptamer Biosensor for Adenosine Triphosphate Detection on a 64 Channel Gold Multielectrode Array, physica status solidi (a), 217(2020) 1900925.

[31] Y. Zhang, G. Figueroa-Miranda, C. Wu, D. Willbold, A. Offenhäusser, D. Mayer, Electrochemical dual-aptamer biosensors based on nanostructured multielectrode arrays for the detection of neuronal biomarkers, Nanoscale, 12(2020) 16501-13.

[32] N. Adly, S. Weidlich, S. Seyock, F. Brings, A. Yakushenko, A. Offenhäusser, et al., Printed microelectrode arrays on soft materials: from PDMS to hydrogels, npj Flexible Electronics, 2(2018) 15.

[33] J. Schnitker, N. Adly, S. Seyock, B. Bachmann, A. Yakushenko, B. Wolfrum, et al., Rapid Prototyping of Ultralow-Cost, Inkjet-Printed Carbon Microelectrodes for Flexible Bioelectronic Devices, Advanced Biosystems, 2(2018) 1700136.

[34] Y. Liang, T. Guo, L. Zhou, A. Offenhäusser, D. Mayer, Label-Free Split Aptamer Sensor for Femtomolar Detection of Dopamine by Means of Flexible Organic Electrochemical Transistors, Materials, 13(2020) 2577.

[35] G. Figueroa-Miranda, L. Feng, S.C.-C. Shiu, R.M. Dirkzwager, Y.-W. Cheung, J.A. Tanner, et al., Aptamer-based electrochemical biosensor for highly sensitive and selective malaria detection with adjustable dynamic response range and reusability, Sensors and Actuators B: Chemical, 255(2018) 235-43.

[36] S. Lee, K.-M. Song, W. Jeon, H. Jo, Y.-B. Shim, C. Ban, A highly sensitive aptasensor towards Plasmodium lactate dehydrogenase for the diagnosis of malaria, Biosensors and Bioelectronics, 35(2012) 291-6.

[37] K.-A. Frith, R. Fogel, J.P.D. Goldring, R.G.E. Krause, M. Khati, H. Hoppe, et al., Towards development of aptamers that specifically bind to lactate dehydrogenase of Plasmodium falciparum through epitopic targeting, Malaria Journal, 17(2018) 191.

[38] J.A. Tanner, Y.W. Cheung, M. Kotaka, U.o.H.K. HKU, Nucleic acid aptamers against plasmodium lactate dehydrogenase and histidine-rich protein ii and uses thereof for malaria diagnosis, (2013).

[39] Y. Lo, Y.-W. Cheung, L. Wang, M. Lee, G. Figueroa-Miranda, S. Liang, et al., An electrochemical aptamer-based biosensor targeting Plasmodium falciparum Histidine-Rich Protein II for malaria diagnosis, Biosensors and Bioelectronics, (2021) 113472.

[40] F. Schröper, D. Brüggemann, Y. Mourzina, B. Wolfrum, A. Offenhäusser, D. Mayer, Analyzing the electroactive surface of gold nanopillars by electrochemical methods for electrode miniaturization, Electrochimica Acta, 53(2008) 6265-72.

[41] A. Kreidenweiss, A.V. Hopkins, B. Mordmüller, 2A and the Auxin-Based Degron System Facilitate Control of Protein Levels in Plasmodium falciparum, PLOS ONE, 8(2013) e78661.

[42] N. Ayawei, A.N. Ebelegi, D. Wankasi, Modelling and Interpretation of Adsorption Isotherms, Journal of Chemistry, 2017(2017) 3039817.

[43] W.J. Peveler, M. Yazdani, V.M. Rotello, Selectivity and Specificity: Pros and Cons in Sensing, ACS Sensors, 1(2016) 1282-5.

[44] L. Feng, Z. Lyu, A. Offenhäusser, D. Mayer, Multi-Level Logic Gate Operation Based on Amplified Aptasensor Performance, Angewandte Chemie International Edition, 54(2015) 7693-7.

[45] E. Katz, V. Privman, Enzyme-based logic systems for information processing, Chemical Society reviews, 39(2010) 1835-57.

[46] G. Hartwich, M. Schneider, A Tunable and Versatile Anchoring System for Gold-Surfaces, Proceedings, 1(2017) 742.

[47] R. Piper, J. Lebras, L. Wentworth, A. Hunt-Cooke, S. Houzé, P. Chiodini, et al., Immunocapture diagnostic assays for malaria using Plasmodium lactate dehydrogenase (pLDH), The American Journal of Tropical Medicine and Hygiene, 60(1999) 109-18.

[48] S.K. Martin, G.-H. Rajasekariah, G. Awinda, J. Waitumbi, C. Kifude, Unified Parasite Lactate Dehydrogenase and Histidine-Rich Protein ELISA for Quantification of Plasmodium falciparum, The American Journal of Tropical Medicine and Hygiene, 80(2009) 516-22.

**Figures**

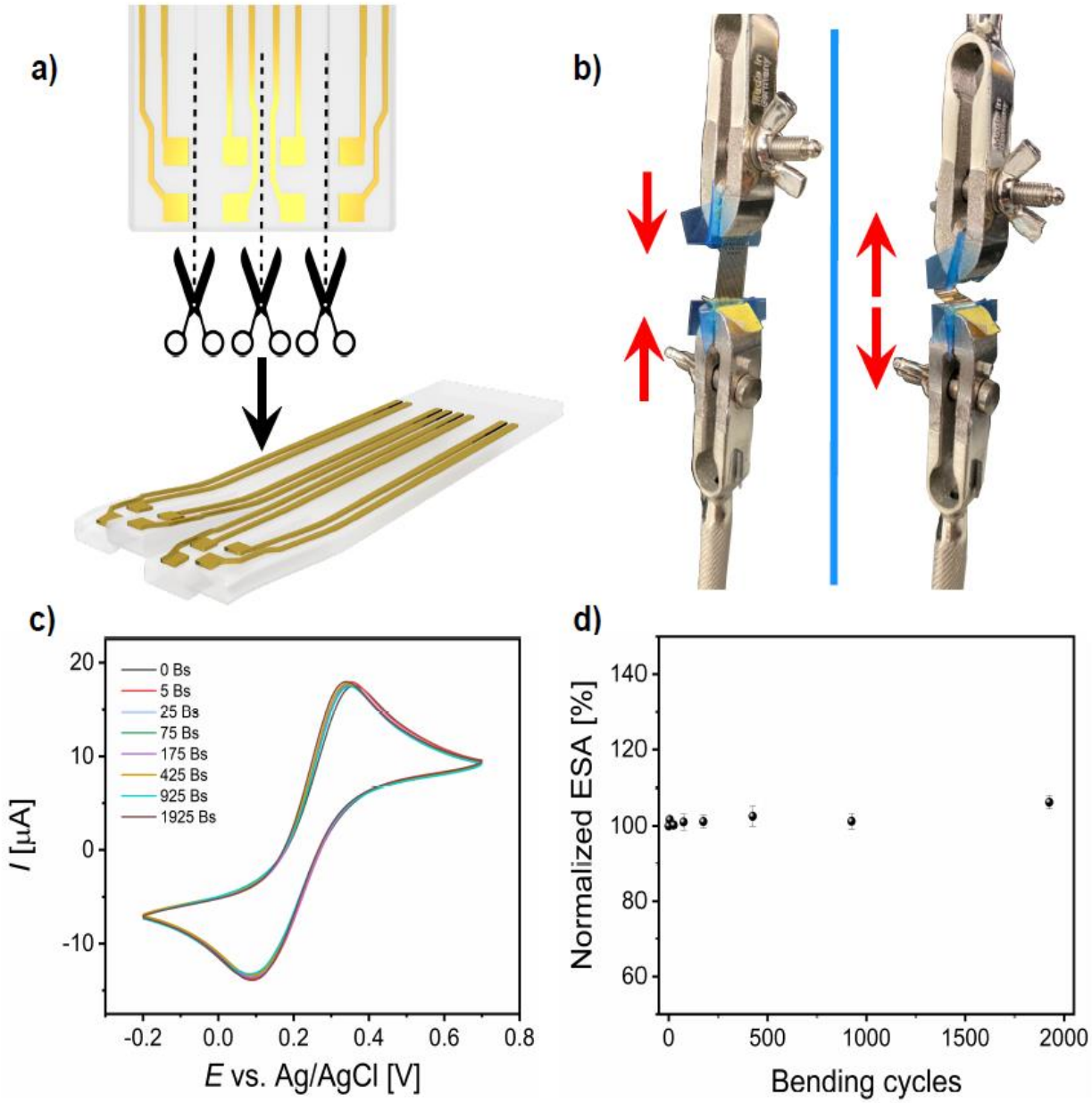


**Fig. 1.** flex-MEA mechanical and electrochemical characterization. a) Schematic representation of the flexible MEA chip, which allows partially divide it into sets of electrodes. b) Mechanical bending test for flex-MEA. c) Characterization of the electrodes before (0 Bs) and after several bending repetitions (5, 25, 75, 175, 425, 925, and 1925 Bs) by cyclic voltammetry in 5 mM $[Fe(CN)_6]^{3-/4-}$ solution at pH 7.5. d) Normalized calculated electrochemical surface area (ESA) after the respective bending cycles.

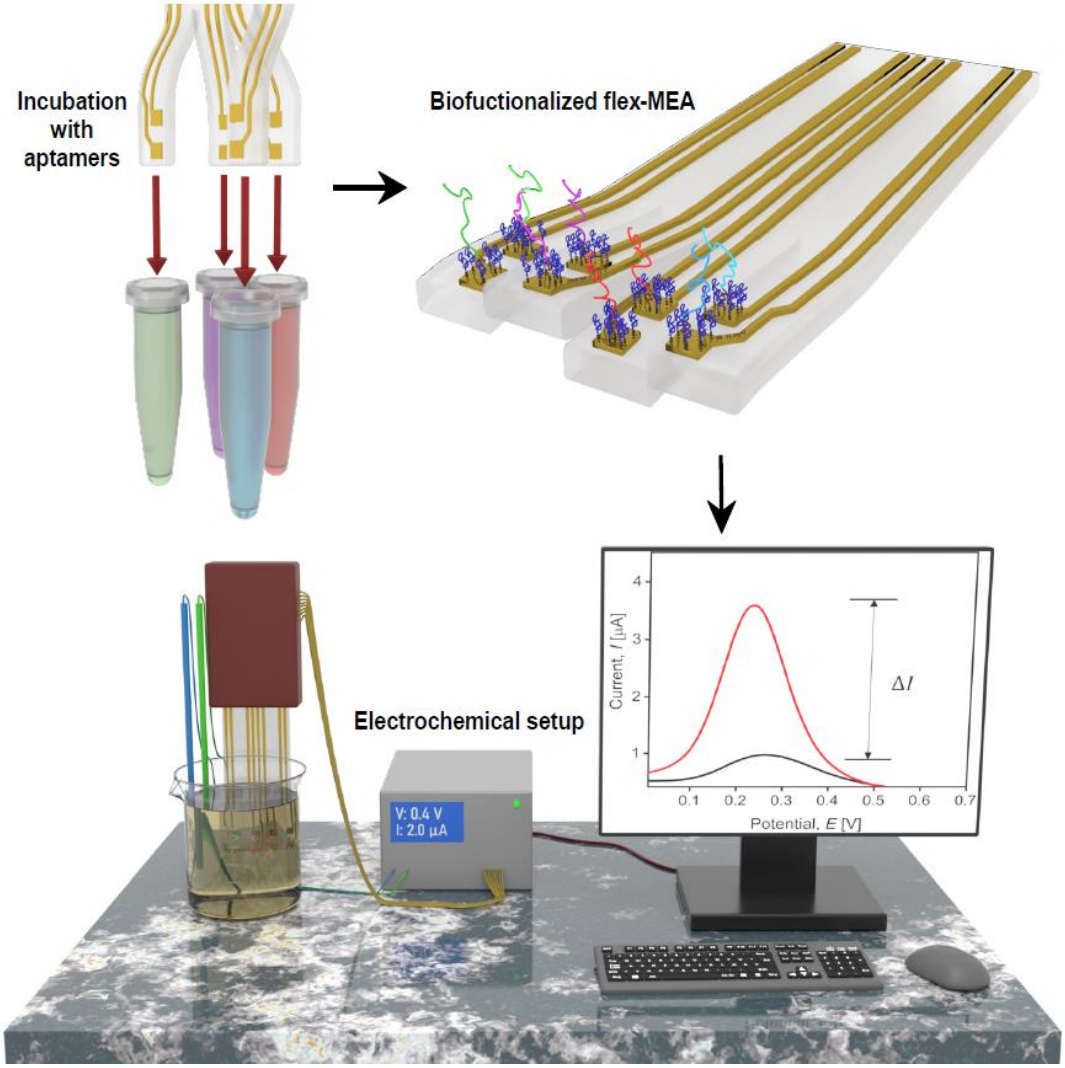


**Fig. 2.** flex-MEA multi-target biofunctionalization and target detection. Schematic representation of the flex-MEA biofunctionalized with the four different aptamers: 2008s (green), pL1 (purple), LDHp11 (red), and 2106s (blue), and the electrochemical setup used for the biosensor characterization. The plot depicts the peak current change ($\Delta I$) between the voltammograms before and after target detection obtained from DPV measurements.

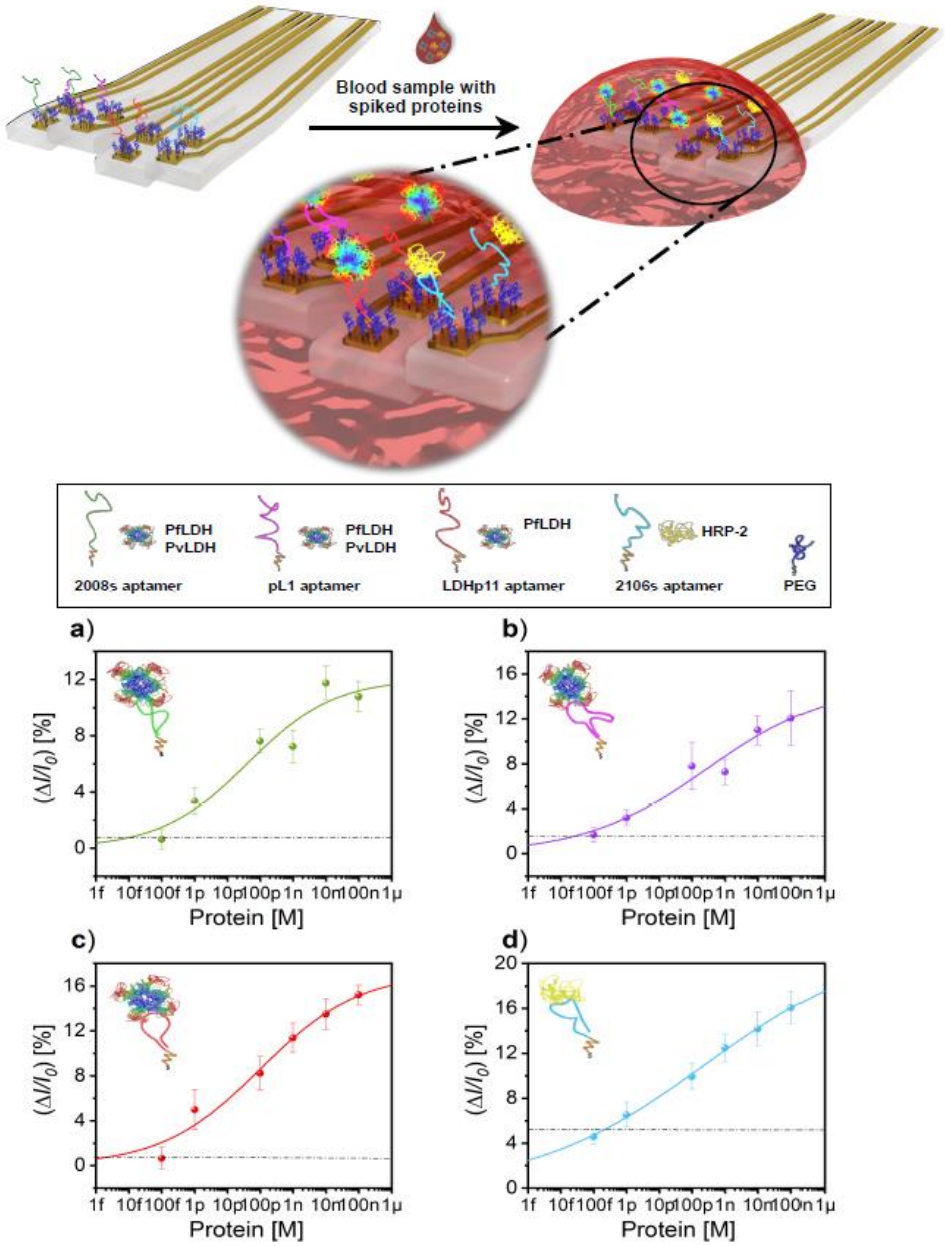


**Fig. 3.** Schematic representation and calibration curves with spiked target analytes in blood samples. The PfLDH target protein was detected by a) 2008s aptamer, b) pL1 aptamer, and c) LDHp11 aptamer. The HRP-2 protein was detected by d) 2106s aptamer. Each plot depicts the normalized percentual signal as function of the protein concentration. All proteins were tested in the concentration range from 100 fM to 100 nM. The dashed line indicates the respective LOD. The experimental data were fitted by a Langmuir-Freundlich adsorption isotherm (equation 1). All experiments were repeated with three different fabricated flex-MEA multi-target aptasensors with different generated sets of electrodes with an n > 6 electrodes for each aptamer.

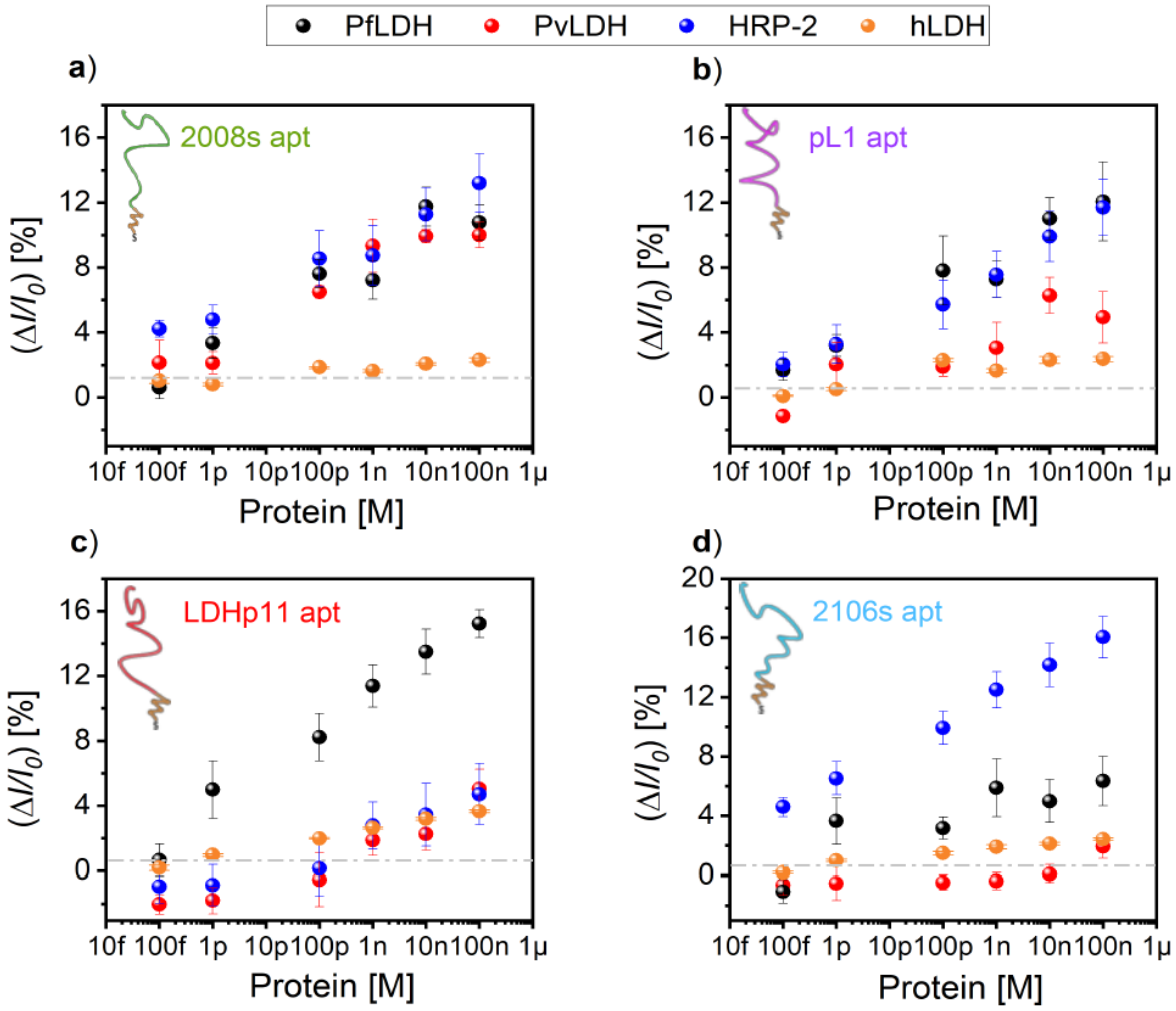


**Fig. 4.** Tests of the cross-selectivity of aptamers versus target proteins. Aptasensors a) 2008s, b) pL1, c) LDHp11, and d) 2106s were tested for binding to individual blood samples spiked with PfLDH, PvLDH, HRP-2, or control human LDH (hLDH). The grey dashed line represents the limit of detection. All experiments were repeated with three different fabricated flex-MEA multi-target aptasensors.

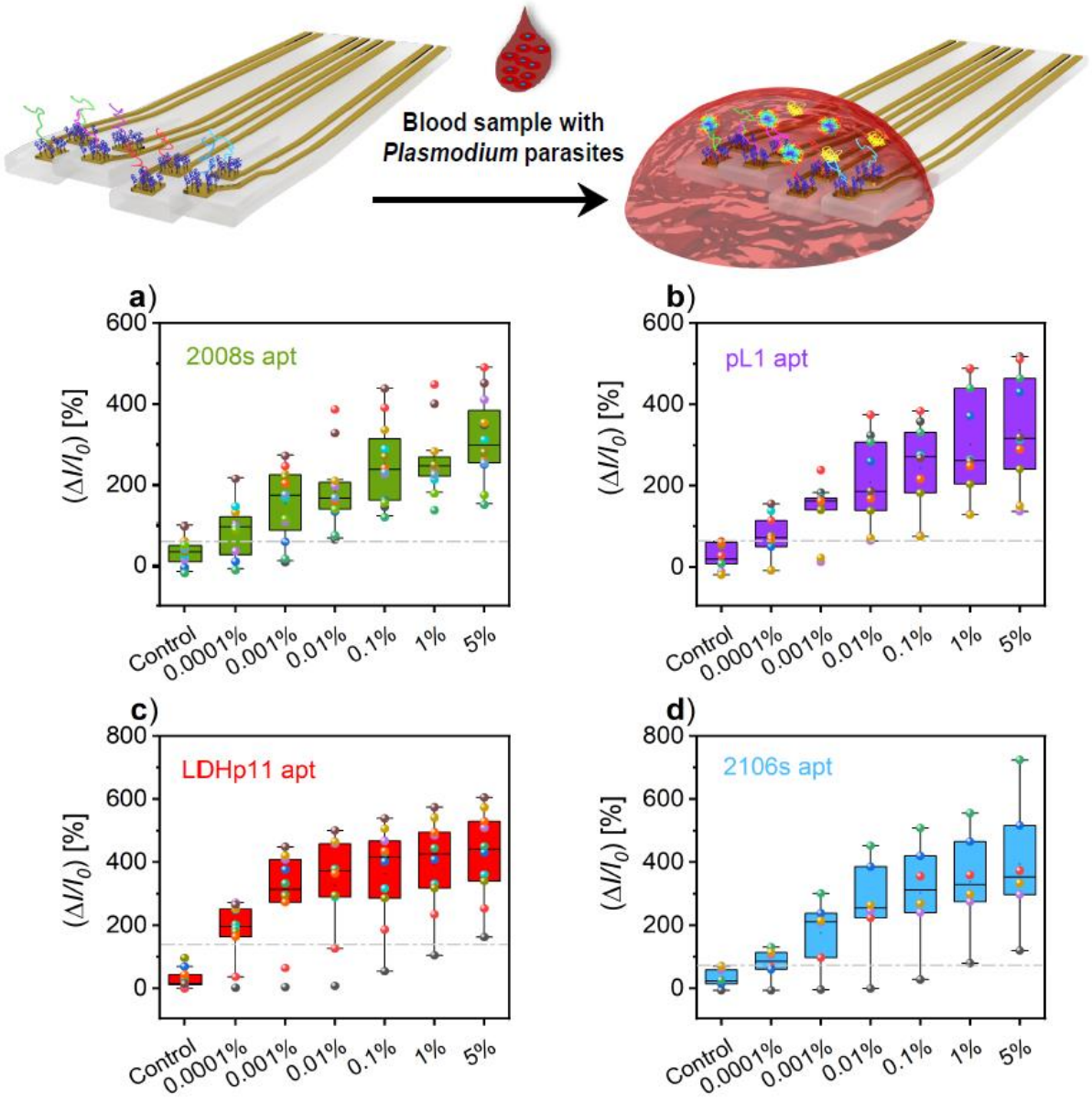


**Fig. 5.** Schematic representation and detection of specific biomarkers in samples of *Plasmodium falciparum* parasite culture. a) 2008 aptamer (green), b) pL1 aptamer (purple), c) LDHp11 aptamer (red) and d) 2106s aptamer (blue). The circles with the same color were measured by the same aptasensor with different percentages of parasitemia. The % represents the percent of parasitemia. All experiments were repeated with three different fabricated flex-MEA multi-target aptasensors with different generated sets of electrodes with an n > 6 electrodes for each aptamer.